

# Superconducting clusters and phase separation in $\text{Pr}_{1+x}\text{Ba}_{2-x}\text{Cu}_3\text{O}_{7+\delta}$ : A $^{63,65}\text{Cu}$ nuclear quadrupole resonance and zero-field NMR study

B. Grévin and Y. Berthier

*Laboratoire de Spectrométrie Physique, Université Joseph-Fourier Grenoble I, Boîte Postale 87,  
38402 Saint Martin d'Hères Cedex, France*

P. Mendels

*LPS URA2 CNRS, Université Paris Sud, 91405 Orsay Cedex, France*

G. Collin

*Laboratoire Léon Brillouin, CEA-Saclay, 91191 Gif sur Yvette Cedex, France*

(Received 21 October 1998; revised manuscript received 23 July 1999)

We present a study on the effect of the  $\text{Pr}^{3+}$  substitution for  $\text{Ba}^{2+}$  in the  $\text{Pr}_{1+x}\text{Ba}_{2-x}\text{Cu}_3\text{O}_{7+\delta}$  system, where small superconducting fractions have been observed in some of the samples with  $x$  in the range  $0.1 < x < 0.6$ . Copper nuclear quadrupole resonance (NQR) and zero-field NMR are reported for the  $x=0.3$  sample  $\text{Pr}_{1.3}\text{Ba}_{1.7}\text{Cu}_3\text{O}_{7+\delta}$  in which the largest superconducting fraction has been detected below 90 K.  $^{63,65}\text{Cu}$  NQR in this sample shows the presence of a fraction of metallic copper in the  $\text{CuO}_2$  planes and confirms that the substitution of Pr onto Ba sites leads to oxygen interchain sites O(5) occupancy. The existence of two different magnetic Cu(2) sites is evidenced for  $x=0.3$  from the comparison of the Cu(2) zero-field NMR in the  $x=0$  and  $x=0.3$  samples. The whole set of results is interpreted in the framework of a phase separation mechanism in the  $\text{CuO}_2$  planes induced by the Ba/Pr substitution. Three characteristic domains are involved, in which respectively localized holes are present, no holes are transferred, and mobile holes reside. We present a model where the observed superconductivity is due to a segregation of local defects in the structure which gives a distribution of clusters containing mobile holes. A local weakening of the  $\text{Pr}_{4f}\text{-O}_{2p}$  hybridization by the Pr/Ba substitution is argued to explain the presence of these clusters.

## I. INTRODUCTION

The possibility of superconductivity in  $\text{PrBa}_2\text{Cu}_3\text{O}_7$  (Pr-123), which has been considered up to now as an insulator, is currently a very active field of research. A large number of experimental and theoretical works have been devoted to give a consistent picture of the insulating state of this compound. The earlier attempt to understand this anomaly in the  $\text{RBa}_2\text{Cu}_3\text{O}_7$  ( $R$ =rare earth) family of cuprates has been the investigation of the  $\text{Y}_{1-x}\text{Pr}_x\text{Ba}_2\text{Cu}_3\text{O}_7$  system in which the superconducting critical temperature decreases progressively as a function of  $\text{Pr}(x)$  concentration and disappears for a critical value  $x_c \geq 0.55$ . Several models have been proposed: magnetic pair breaking by Pr,<sup>1</sup> hole-filling<sup>1</sup> by  $\text{Pr}^{4+}$ , chain-disorder induced by Ba/Pr substitution<sup>2</sup> and hole localization in  $\text{Pr}_{4f}\text{-O}_{2p\pi}$  orbitals.<sup>3,4</sup> The three first models fail to consistently explain a large number of experimental observations. In the last one proposed by Fehrenbacher and Rice<sup>3</sup> the holes are effectively doped in  $\text{CuO}_2$  planes, but are localized in  $\text{Pr}_{4f}\text{-O}_{2p\pi}$  orbitals. This assumption has been confirmed by many studies such as x-ray absorption experiments,<sup>5</sup>  $^{17}\text{O}$  NMR,<sup>6</sup> or charge density study<sup>7</sup> and has been up to now widely accepted as the most plausible model to explain the lack of superconductivity in Pr-123. Nevertheless neither the progressive decreasing of  $T_c$  in the  $\text{Y}_{1-x}\text{Pr}_x\text{Ba}_2\text{Cu}_3\text{O}_7$  system nor the recent reports on superconductivity in Pr-123 thin films<sup>8,9</sup> and crystals<sup>10,11</sup> are explained by this model alone. Concerning the last point, the situation is especially

complicated by the lack of consensus concerning the synthesis conditions leading to superconductivity in Pr-123. On the one hand, some authors<sup>8,11</sup> have emphasized the role of disorder induced by  $\text{Pr}^{3+}$  on the  $\text{Ba}^{2+}$  sites, and concluded that the key to obtaining superconducting Pr-123 was to prepare samples under synthesis conditions that minimize the amount of  $\text{Pr}^{3+}$  on  $\text{Ba}^{2+}$  sites. In this way, Blackstead *et al.*<sup>8</sup> have reported the observation of inhomogeneous superconductivity (detected by surface resistance measurements at microwave frequencies) below  $T_c \approx 90$  K in thin films, and a Meissner effect has been observed by Shukla *et al.*<sup>11</sup> below the same temperature in small crystallites. On the other hand, bulk superconductivity (associated with zero resistivity at low temperatures) has been observed by Zou *et al.* only in the case of inhomogeneous samples,<sup>10</sup> in which there is a doubt about the oxygen stoichiometry and the degree of Ba-Pr substitution. Moreover, in these samples,  $T_c$  is smaller ( $\sim 80$  K at ambient pressure) than that reported for well-ordered samples, and is anomalously enhanced under pressure.<sup>12</sup>

Independently of the effect of the synthesis conditions on the superconducting character of Pr-123 samples, Cao *et al.*<sup>13</sup> have pointed out the crucial role of Ba substitution by isovalent Sr ion, on the restitution of superconductivity, in an initially nonsuperconducting  $\text{Y}_{0.4}\text{Pr}_{0.6}\text{Ba}_2\text{Cu}_3\text{O}_7$  sample. Both metallic conductivity and superconductivity were observed in  $\text{Y}_{0.4}\text{Pr}_{0.6}\text{Ba}_{2-x}\text{Sr}_x\text{Cu}_3\text{O}_7$  at  $x \geq 0.75$ , accompanied by an orthorhombic to tetragonal transition. More recently

Muroi *et al.*<sup>14</sup> underlined the inhomogeneous character of the superconductivity observed in the  $Y_{1-x}Pr_xBa_{2-y}Sr_yCu_3O_7$  system, arguing that the main effect of Sr substitution for Ba, was the weakening of the  $Pr_{4f}-O_{2p}$  hybridization near the substituted site through a local structure change.

In the present work we show that the effect of Ba partial substitution by Pr in the Pr-123 system can generate superconducting clusters and we study the mechanism of phase separation which is present in the  $CuO_2$  planes. Varying the Pr concentration in the  $Pr_{1+x}Ba_{2-x}Cu_3O_{7+\delta}$  system from  $x=0$  to  $x=0.6$  (the limit of solubility), we observed the greatest fraction of superconductivity for  $x=0.3$ . We focus our study on the two samples (fully oxygenated) with  $x=0$  where no superconductivity was detectable and  $x=0.3$  in which a significant superconducting fraction was extracted below  $T_c \sim 90$  K from SQUID susceptibility measurements. For this investigation we have used NQR and zero-field NMR as local probes ideally suited for the observation of the electronic state and the environment of copper atoms in the Cu(1) chain sites and Cu(2) plane sites. NQR is sensitive to the local electric field gradient (EFG) value, and provides valuable information about ionicity, bonding and local charge state. The zero-field NMR spectra which are typical of well defined magnetic local structures, give a direct estimate of the local hyperfine magnetic field  $H_{hf}$  and EFG values on Cu(2) site in the AF ordered state of  $CuO_2$  planes.

From copper NQR measurements in the sample with  $x=0.3$  (see Sec. IV B), *metallic Cu(2) sites* were identified in the  $CuO_2$  planes *whose low density corresponds to the fraction of superconductivity* detected by susceptibility measurements. We also observed various oxygen coordinations of the chain copper sites and particularly the oxygen antichain sites O(5) occupancy. For the analysis of these result, we used a comparison with the copper NQR spectrum in the  $La_{1.3}Ba_{1.7}Cu_3O_{7+\delta}$  compound which is isostructural to  $Pr_{1.3}Ba_{1.7}Cu_3O_{7+\delta}$  but exhibits bulk superconductivity ( $T_c = 48$  K).

In addition to the presence of a small fraction of metallic Cu(2) sites, we observed using copper zero-field NMR in  $Pr_{1.3}Ba_{1.7}Cu_3O_{7+\delta}$  (see Sec. IV C) *two other distinct Cu(2) sites characterized by different local hyperfine field values*. These findings microscopically demonstrate the presence of an in-plane magnetic phase separation. Furthermore the copper zero-field NMR spectra measured in fully doped  $PrBa_2Cu_3O_7$  and in oxygen-depleted  $PrBa_2Cu_3O_{6.9}$  are compared with those reported in the literature for  $PrBa_2Cu_3O_{6+x}$  (Ref. 15) and  $Y_1Ba_2Cu_3O_6$ .<sup>16,17</sup> This comparison gives evidence for a strong sensitivity of this data to the oxygen stoichiometry.

We show (in Sec. V) that *the three types of planar Cu sites arise from distinct structural environments involving the various oxygen coordinations of the chain copper sites and the substitution of Pr onto Ba sites*; these enable charge transfer between chains and planes that produce various hole doping situations in the planes (so-called alpha, beta and gamma sites). We discuss the occurrence of local superconductivity in the framework of microphase separation in the  $CuO_2$  planes induced by Pr substitution on Ba sites and the formation of clusters where the charge transfer from chains to planes is active while the  $Pr_{4f}-O_{2p}$  hybridization is suppressed. Finally we briefly discuss the connection of our re-

sults with previous work bearing on phase separation in cuprates.

The paper is organized as follows. The next section reviews the NQR/zero-field NMR background necessary to understand results and discussion. Section III provides some information on the experimental techniques including the characterization of samples. In Sec. IV we present and analyze our data obtained by susceptibility measurements (Sec. IV A), copper NQR (Sec. IV B) and zero-field NMR (Sec. IV C), followed by a discussion in Sec. V and a summary in Sec. VI.

## II. ZERO-FIELD NMR AND NQR THEORETICAL BACKGROUND

In NMR experiments, one considers the interaction between the nuclear spin  $I$  and (i) the static applied magnetic field  $H_0$ , (ii) the local hyperfine magnetic field, and (iii) the local electric field gradient (EFG). The total Hamiltonian of the nuclear spin  $I$  can be written as

$$H = H_{\text{Zeeman}} + H_{\text{hyperfine}} + H_{\text{quadrupole}}, \quad (1)$$

with

$$H_{\text{Zeeman}} = -\gamma_n \hbar \vec{H}_0 \cdot \vec{I} \quad (2)$$

and

$$H_{\text{quadrupole}} = \frac{eQV_{zz}}{4I(2I-1)} \left[ 3I_z^2 - I^2 + \frac{\eta}{2}(I_+^2 + I_-^2) \right]. \quad (3)$$

We do not discuss the hyperfine Hamiltonian in detail, as it does not contribute directly to NQR spectra, and since usually  $H_0$  is set equal to  $H_{\text{int}}$  in the Zeeman Hamiltonian to account for the static part of the internal field  $H_{\text{int}}$  in zero-field NMR experiments. In the case of NQR, one sets  $H_0 = 0$ , and the quadrupole part of the Hamiltonian gives rise to doubly degenerate energy levels. In the particular case of Cu with  $I=3/2$ , a single NQR line is observed for the two isotopes  $^{63}\text{Cu}$  (69%) and  $^{65}\text{Cu}$  (31%):

$${}^{63,65}\nu_Q = \frac{{}^{63,65}QeV_{zz}}{2h} \sqrt{1 + \frac{\eta^2}{3}}, \quad (4)$$

where  $Q$  stands for the nuclear quadrupole moment,  $V_{\alpha\alpha}$  ( $\alpha=x,y,z$ ) for the principal components of the local electric field gradient tensor  $V$ , and  $\eta = (V_{xx} - V_{yy})/V_{zz}$  is the asymmetry parameter of the EFG. A doublet is therefore expected for the  $^{63,65}\text{Cu}$  NQR line, with frequencies corresponding to the ratio of the nuclear quadrupole moments  ${}^{63}Q/{}^{65}Q = 1.08$ , and with amplitudes in the ratio of natural isotopic relative abundances  ${}^{65}\text{A}/{}^{63}\text{A} = 0.45$ .

In crystalline solids, the EFG is usually described by on-site and lattice contributions:

$$eQ = (1 - \gamma_\infty)eQ^{\text{lattice}} + (1 - R_Q)eQ^{\text{on-site}} \quad (5)$$

( $\gamma_\infty$  and  $R_Q$  are the Sternheimer anti-shielding factors; for more details see Ref. 18). In the particular case of copper in high- $T_c$  superconductors, the NQR frequency is sensitive to two factors: the first is related to the Cu oxygen environment, and the second to the hole density in the Cu-O orbitals. The first effect mainly concerns the Cu(1) chain site (see Fig. 1).

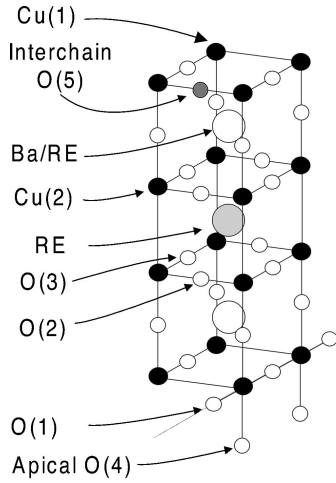


FIG. 1. Schematic drawing of the  $R_{1+x}\text{Ba}_{2-x}\text{Cu}_3\text{O}_{7+\delta}$  structure (the buckling of  $\text{CuO}_2$  planes is not represented). Light  $R^{3+}$  ions are known to be soluble on  $\text{Ba}^{2+}$  sites, leading to oxygen O(5) antichain occupancy.

In  $R\text{Ba}_2\text{Cu}_3\text{O}_7$ , three neighboring configurations for the Cu(1) site are possible with twofold, threefold, and fourfold oxygen coordinations, each being characterized by a narrow range of NQR frequencies, which can slightly vary depending on the RE ionic size.<sup>16,19,20</sup> For example, one gets  $^{63}\nu_Q$  values between 30.2 MHz and 29.9 MHz for Cu(1)-O2 sites, whereas Cu(1)-O4 in full chains are characterized by lower values, ranging from 21.8 MHz to 23 MHz (for more details, see Lütgemeier *et al.*<sup>20</sup>). On the other hand, in the case of the Cu(2) plane site with the coordination Cu(2)-O4, band structure calculations have shown that the EFG is sensitive to on-site contributions.<sup>22–24</sup> Zheng *et al.* have given a detailed analysis of Cu(2)  $^{63}\nu_Q$  values reported for different high- $T_c$  superconductors.<sup>25</sup> They concluded that the hole-density in Cu  $3d_{x^2-y^2}$  and O  $2p_\sigma$  orbitals are key parameters, which are to be considered to account for the Cu(2) EFG variations from one high- $T_c$  superconductor to the others. Last of all, we want to underline the fact that in the case of Cu(1) in full-oxygenated chains, the hole-doping level of the Cu-O orbitals should be considered in a way similar to that used by Zheng *et al.* for the analysis of the Cu(2) EFG. The Cu(1) quadrupolar frequency is very sensitive to the doping level of  $\text{CuO}_3$  chains, as shown by the comparison between the value in Y-123 hole-doped chains [ $\sim 0.5$  hole per Cu(1) in the  $3d^9$  configuration, and  $^{63}\nu_Q \approx 22.2$  MHz at 300 K in this study] and the lower one obtained by Takigawa<sup>26</sup> *et al.* in the quasi-isostructural *insulating* chain of  $\text{Sr}_2\text{CuO}_3$  [Cu(1) in the  $3d^9$  configuration, and  $^{63}\nu_Q \approx 3.7$  MHz at 280 K].

In zero applied field NMR experiments, the static field in the Hamiltonian is equal to the local internal magnetic field,  $H_0 = H_{\text{int}}$ , and thus  $H_{\text{quadrupole}} \ll H_{\text{Zeeman}}$ . For each Cu isotope, a central line is expected from the  $(+\frac{1}{2}, -\frac{1}{2})$  transition, and two satellite lines from the  $(\pm\frac{1}{2}, \pm\frac{3}{2})$  transitions. The central line frequencies for  $^{65}\text{Cu}$  and  $^{63}\text{Cu}$  are in the ratio of the magnetic moment of the two isotopes:  $^{65}\gamma/^{63}\gamma = 1.07$ , resulting in a higher frequency for the  $^{65}\text{Cu}$  lines. Six peaks are therefore observed resulting from the quadrupolar splitting of  $^{63}\text{Cu}$  and  $^{65}\text{Cu}$  Zeeman levels, generally overlapping each other, with amplitudes and frequencies that depend on the relative values of  $H_{\text{int}}$  and  $\nu_Q$ . In principle, a careful

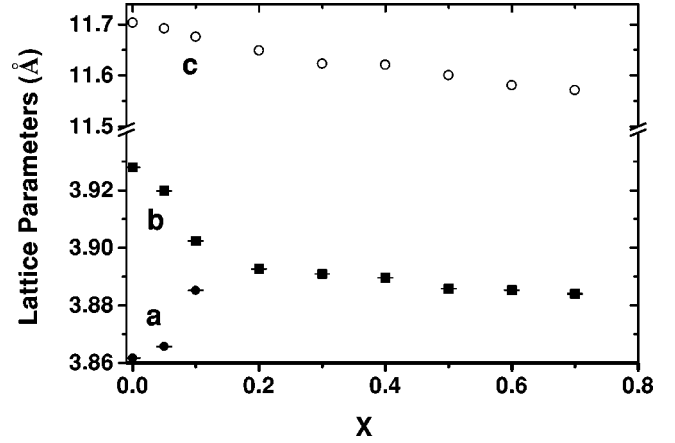


FIG. 2. Lattice constant parameters (in Å) of our  $\text{Pr}_{1+x}\text{Ba}_{2-x}\text{Cu}_3\text{O}_{7+\delta}$  samples: **a** (full circles), **b** (squares), and **c** (open circles) as a function of Pr concentration. Standard deviations are included in symbols.

analysis of zero-field NMR spectra allows the values of  $H_{\text{int}}$  and  $\nu_Q$  to be extracted, as well as the angle  $\theta$  between  $H_{\text{int}}$  and the  $c$  axis.

### III. EXPERIMENTAL DETAILS

#### A. Sample preparation

Our experiments were carried out on powdered samples. The  $\text{PrBa}_2\text{Cu}_3\text{O}_7$  sample was carefully prepared in order to avoid Pr/Ba substitution and oxygen defects on the chains as previously described in Ref. 27. The effects of a systematic substitution of barium by praseodymium in  $\text{Pr}_{1+x}\text{Ba}_{2-x}\text{Cu}_3\text{O}_{7+\delta}$  have been studied for  $0.1 < x < 0.6$ . The main difference in the synthesis process concerns the higher temperature of reaction in air between the three oxides  $\text{Pr}_6\text{O}_{11}$ ,  $\text{BaO}_2$ , and  $\text{CuO}$ , which varies from 930 °C for  $x = 0$  to 990 °C for  $x = 0.6$ . The evolution of the lattice parameters as a function of  $x$ , obtained from a Rietvelt adjustment of the x-ray diffraction patterns (Cu  $K\alpha$ ), is shown in Fig. 2. The transition from an orthorhombic to tetragonal structure occurs for  $0.1 < x < 0.2$ , and the limit of the solid solution is reached for  $x > 0.6$ , in agreement with previous diffraction studies.<sup>28,29</sup> A similar procedure of synthesis was used for the  $\text{La}_{1.3}\text{Ba}_{1.7}\text{Cu}_3\text{O}_{7+\delta}$  sample and the tetragonal structure is also demonstrated with  $a = 3.9101(1)$  Å and  $c = 11.7485(5)$  Å. Finally,  $\text{PrBa}_2\text{Cu}_3\text{O}_{6.9}$  (oxygen depleted) and  $\text{YBa}_2\text{Cu}_3\text{O}_7$  ( $T_c^{\text{midpoint}} \sim 89.5$  K) samples were obtained by conventional preparation methods.

#### B. NQR and zero-field NMR spectroscopies

The zero-field NMR and NQR experiments were performed using a standard pulse spectrometer. In NQR and zero-field NMR experiments, the quantization axis for the nuclear energy levels are respectively given by the principal axis of the EFG tensor and the local internal field direction. This allows accurate studies on powders, as there is no line broadening due to the axis orientation dispersion, contrary to the case of NMR experiments. Zero-field NMR and NQR  $^{63,65}\text{Cu}$  spectra were obtained plotting the integral of the ech-

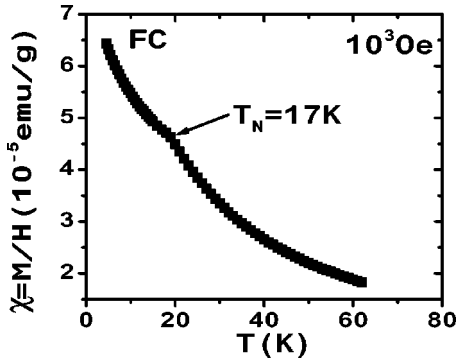


FIG. 3. SQUID susceptibility measurements in  $\text{PrBa}_2\text{Cu}_3\text{O}_7$  under  $10^3$  Oe (field cooled mode).

oes versus the applied radio frequency (rf) after a  $\pi/2 - \tau - \pi$  rf pulse sequence. The spin-echo signal was averaged at least  $10^3$  times, in order to increase the signal to noise ratio and a phase alternation of the rf pulses was used to obtain a ringing free echo signal. Zero-field NMR and NQR signals were normalized with respect to  $1/\omega_L^2$ , where  $\omega_L$  is the Larmor frequency. The Cu(1) NQR spectra were obtained between 4.2 K and 300 K, whereas the Cu(2) zero-field NMR spectra were obtained below 4.2 K, owing to the increase in spin-spin relaxation rate  $1/T_2$  at higher temperatures [this rate, when given as in Fig. 9(b), was estimated by a single exponential fit].

### C. SQUID susceptibility measurements

Zero-field-cooled (ZFC) and field-cooled (FC) magnetic susceptibility measurements were performed using a SQUID susceptometer for different low applied magnetic fields (few Gauss to 100 Gauss, depending on the sample under investigation). This allowed one to single out the superconducting transition temperature and the screening fraction in a reliable manner. Indeed for higher fields, the paramagnetic-like contribution due to Pr ions, which is proportional to field, overcomes and masks the superconducting contribution, which, on the contrary, decreases with increasing field.

## IV. EXPERIMENTAL RESULTS AND ANALYSIS

### A. Susceptibility measurements

Systematic susceptibility measurements were performed on all our  $\text{Pr}_{1+x}\text{Ba}_{2-x}\text{Cu}_3\text{O}_{7+\delta}$  fully oxygenated samples for  $x$  varying between  $x=0$  and  $x=0.6$  in order to search for bulk superconductivity in relation to the Pr/Ba substitution. For  $x \geq 0.4$  no trace of superconductivity was observed, which is in contrast with  $x < 0.4$  where some samples presented traces of superconductivity. Only one batch, for  $x=0.3$ , yielded a sizeable diamagnetic contribution of 0.2%. We discuss next the  $x=0$  and  $x=0.3$  cases which have been studied in great detail.

The susceptibility curve  $\chi(T) \equiv M/H$  for  $\text{PrBa}_2\text{Cu}_3\text{O}_7$  under  $H=10^3$  Oe (FC mode) is shown in Fig. 3. The curve exhibits a deflection point at  $T_N \approx 17 \pm 1$  K, which is easily attributed to Pr AF ordering. This result is in good agreement with other studies<sup>1</sup>. In the case of  $\text{Pr}_{1.3}\text{Ba}_{1.7}\text{Cu}_3\text{O}_{7+\delta}$ , a diamagnetic effect is present below 90 K, and a *negative Meissner effect* is clearly deduced from the typical curves obtained

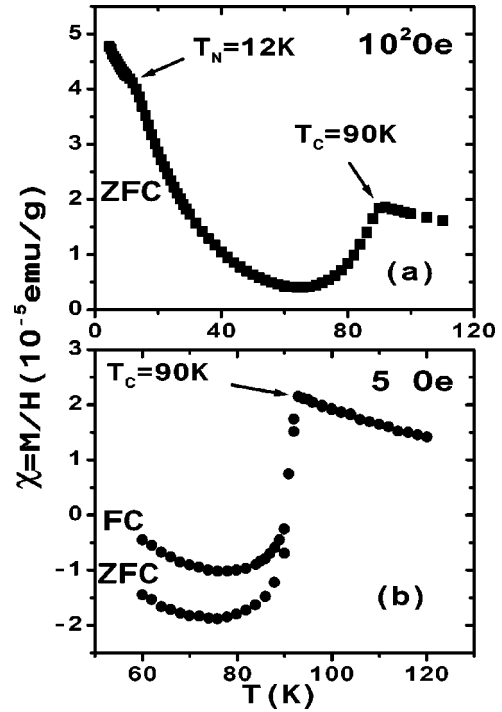


FIG. 4. SQUID susceptibility measurements in  $\text{Pr}_{1.3}\text{Ba}_{1.7}\text{Cu}_3\text{O}_{7+\delta}$ : (a) ZFC under  $10^2$  Oe (black squares) and (b) FC and ZFC under 5 Oe (filled circles).

for  $H=5$  Oe (ZFC and FC, Fig. 4). Here, the negative value of the magnetization below  $T_c$  dominates the paramagnetic Pr contribution in the temperature range  $90 \text{ K} > T > 70 \text{ K}$ . This allows a direct estimate of the superconducting fraction, and we deduce the values of the order of 0.2% for the shielding fraction (ZFC) and of 0.08% for the Meissner fraction (FC), under 5 Oe. Other fields up to 100 G yielded similar shielding fractions whereas the Meissner effect was found to decrease by a factor  $\sim 4$  between 1 and 100 G. The signature of the Pr lattice magnetic ordering at  $T_N \approx 12$  K can also be observed. We conclude that a very small fraction undergoes a superconducting transition below 90 K in the  $x=0.3$  sample, whereas no sizeable effect was observed in the  $x=0$  sample.

It is worth noting that for a similar composition for the rare earth ions, the  $\text{La}_{1.3}\text{Ba}_{1.7}\text{Cu}_3\text{O}_{7+\delta}$  system exhibits bulk superconductivity at much lower temperature ( $T_c = 48 \pm 1$  K), with a superconducting fraction roughly equal to 50% (corresponding to a susceptibility decrease of  $6 \times 10^{-3}$  emu/g).

### B. $^{63,65}\text{Cu}$ copper NQR

#### 1. The Cu NQR spectrum of the $\text{PrBa}_2\text{Cu}_3\text{O}_7$ sample ( $x=0$ )

The  $^{63,65}\text{Cu}(1)$  spectra at 300 K and 4.2 K in  $\text{PrBa}_2\text{Cu}_3\text{O}_7$  are shown in Fig. 5. A doublet is expected for the NQR line, with frequencies corresponding to the ratio of the nuclear quadrupole moments,  $^{63}\text{Q}/^{65}\text{Q} = 1.08$ , of the two isotopes  $^{63}\text{Cu}$  (69%) and  $^{65}\text{Cu}$  (31%), and in the absence of metallic Cu(2) sites the frequency range of the whole NQR spectrum is limited to the usual range 19–24 MHz. However, the line shape is strongly broadened at low temperatures, mainly due to a charge density wave occurring in the  $\text{CuO}_3$

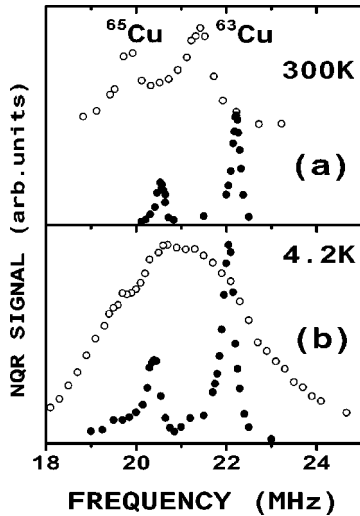


FIG. 5.  $^{63,65}\text{Cu}(1)$  NQR spectra at 300 K (a) and 4.2 K (b) in  $\text{Pr}_1\text{Ba}_2\text{Cu}_3\text{O}_7$  (open circles) and in  $\text{YBa}_2\text{Cu}_3\text{O}_7$  (filled circles). The origin of the vertical scale of the  $\text{Pr}_1\text{Ba}_2\text{Cu}_3\text{O}_7$  spectrum at 300 K is shifted up for clarity.

chain below 120 K, as reported in a previous paper.<sup>27</sup> In an earlier study, Nehrke *et al.*<sup>30</sup> reported a large  $^{63,65}\text{Cu}(1)$  NQR linewidth, constant between 4.2 K and 25 K, and attributed this effect to crystallographic disorder. Our measurements at 300 K however, show that at higher temperatures, the  $^{63,65}\text{Cu}(1)$  doublet is better resolved. This makes possible a safe comparison to be made between Pr-123 and other  $\text{R}\text{Ba}_2\text{Cu}_3\text{O}_7$  compounds ( $\text{R}=\text{Rare earth}$ ).<sup>20</sup> The value obtained for the quadrupolar frequency ( $^{63}\nu_Q=21.36$  MHz) is not very far from that observed in the  $\text{R}\text{Ba}_2\text{Cu}_3\text{O}_7$  compounds with small rare earth ions like  $\text{YBa}_2\text{Cu}_3\text{O}_7$ . This might seem contradictory with the dependence of the Cu(1) NQR frequency on the ionic radius  $r$  of the rare earth, observed by Lutgemeier *et al.*<sup>20</sup> as Pr presents a larger value of  $r$  than Y. We must in fact recall that in  $\text{Pr}\text{Ba}_2\text{Cu}_3\text{O}_7$  the distance between the different Cu-O layers are severely modified by the Pr-O(2,3) orbital hybridization and this leads to a similar crystallographic environment for the Cu(1) atoms in Y-123 and Pr-123 systems. Following this remark, the NQR frequencies observed confirm that the chain doping in  $\text{Pr}\text{Ba}_2\text{Cu}_3\text{O}_7$  and in  $\text{YBa}_2\text{Cu}_3\text{O}_7$  is similar, bearing in mind that  $^{63}\nu_Q$  for Cu(1) is very sensitive to the hole density in Cu-O orbitals. This result is in good agreement with other studies<sup>31,32</sup> using different techniques.

## 2. NQR spectrum in the substituted $\text{Pr}_{1.3}\text{Ba}_{1.7}\text{Cu}_3\text{O}_{7+\delta}$ sample ( $x=0.3$ )

The  $^{63,65}\text{Cu}$  NQR spectrum observed at 4.2 K in the partially Ba/Pr substituted  $\text{Pr}_{1.3}\text{Ba}_{1.7}\text{Cu}_3\text{O}_{7+\delta}$  sample is shown in Fig. 6. It is highly broadened, and ranges from 17 MHz to 40 MHz revealing new sites when compared to the previous spectrum of  $\text{Pr}\text{Ba}_2\text{Cu}_3\text{O}_7$ . Moreover, the high frequency extension of the spectrum beyond 30 MHz is unusual for Cu(1) sites alone and poses the question of the presence of metallic Cu(2) sites despite the fact that an antiferromagnetic order is observed in the  $\text{CuO}_2$  planes. A natural consequence of this magnetic ordering is that most of the Cu(2) sites must appear at higher frequencies between 80 and 120 MHz due to the characteristic local internal field.

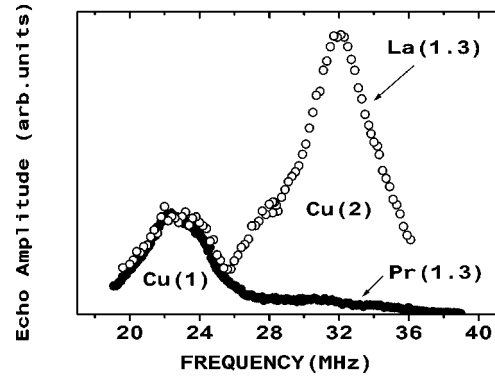


FIG. 6.  $^{63,65}\text{Cu}$  NQR line shape at 4.2 K in  $\text{Pr}_{1.3}\text{Ba}_{1.7}\text{Cu}_3\text{O}_{7+\delta}$  with  $t_{\text{rep}}=25$  msec (full circles). The  $^{63,65}\text{Cu}$  spectrum obtained in  $\text{La}_{1.3}\text{Ba}_{1.7}\text{Cu}_3\text{O}_{7+\delta}$  using the same experimental conditions is represented (open circles) with the echo amplitude normalized at 22 MHz for comparison.

For the assignment of the lines and for the discrimination between Cu(1) and Cu(2) sites we will use a systematic comparison with the spectrum observed in the isostructural superconducting  $\text{La}_{1.3}\text{Ba}_{1.7}\text{Cu}_3\text{O}_{7+\delta}$  compound ( $T_c=48$  K), where the Cu(1) site environments are similar and where superconducting Cu(2) sites exist. The  $\text{La}^{3+}$  ionic radius is close to that of  $\text{Pr}^{3+}$  and its substitution on  $\text{Ba}^{2+}$  sites is supposed to induce the same perturbation on the charge reservoir layer as in  $\text{Pr}_{1.3}\text{Ba}_{1.7}\text{Cu}_3\text{O}_{7+\delta}$ . Furthermore the non-magnetic character of the La sublattice simplifies the spectrum analysis as any extra transferred hyperfine field on the Cu(1) sites is excluded. We will also use the reference of the Cu(1) and Cu(2) spectrum in  $\text{YBa}_2\text{Cu}_3\text{O}_{6+x}$  (Refs. 16 and 19) and in  $\text{LaBa}_2\text{Cu}_3\text{O}_{6+x}$ ,<sup>20,21</sup> where Cu(1) sites having different oxygen coordination have been studied in detail by NQR. In  $\text{YBa}_2\text{Cu}_3\text{O}_{6+x}$  the oxygen coordination dependence on the NQR frequency for the Cu(1) is the following: 30.1 MHz, 24 MHz, and 22.05 MHz for the  $\text{Cu}(1)_2$ ,  $\text{Cu}(1)_3$ , and  $\text{Cu}(1)_4$  sites, respectively, where the subscript denotes the number of oxygen coordination. Furthermore, the  $\text{Cu}(1)_2$  sites present a longer spin lattice relaxation time than the  $\text{Cu}(1)_3$  and  $\text{Cu}(1)_4$  sites. The NQR results obtained by Goto *et al.*<sup>21</sup> in the  $\text{LaBa}_2\text{Cu}_3\text{O}_{6+x}$  system are also of particular interest for our analysis as the substitution of  $\text{La}^{3+}$  ion on the Ba sites was always present in all of their samples and was independent of the oxygen stoichiometry. An extra set of lines, not observed in the other R-123 systems, is present in their spectrum even for  $x=7.06$  at the frequencies of 33 MHz and 30.50 MHz for the two  $^{63,65}\text{Cu}$  isotopes, respectively. These lines could be associated to Cu(2) sites just above a Cu(1) site surrounded by oxygen atoms on the O(5) sites (along the  $a$  direction).

The copper NQR spectra of  $\text{La}_{1.3}\text{Ba}_{1.7}\text{Cu}_3\text{O}_{7+\delta}$  obtained at 4.2 K and for two different repetition times in the spin echo sequence, are presented in Figs. 7(b) and 7(c) together with a typical spectrum of  $\text{LaBa}_2\text{Cu}_3\text{O}_{6.93}$  reported by Lutgemeier *et al.*<sup>20</sup> In the  $\text{La}_{1.3}\text{Ba}_{1.7}\text{Cu}_3\text{O}_{7+\delta}$  spectrum, obtained using a slow repetition rate [Fig. 7(b)], a line appears at 30.2 MHz which is not present when a fast repetition rate is used as in the spectrum in Fig. 7(c). The same feature was typically observed for  $\text{YBa}_2\text{Cu}_3\text{O}_{6.5}$  and reveals the presence of  $\text{Cu}(1)_2$  sites where O(1) neighbors are missing and with

copper atoms in the  $3d^{10}$  configuration. The absence of a magnetic moment on these copper atoms is responsible for the long spin-lattice relaxation rate measured at these sites. The presence of these  $\text{Cu}(1)_2$  sites shows that the substitution of an  $\text{La}^{3+}$  ion on the Ba sites introduces a large disorder in the Cu-O chains and that the number of oxygen atoms on the O(1) sites decreases by a large amount. The higher frequency range of the spectrum between 26 and 37 MHz observed using a fast repetition time (25 msec) can be assigned to the Cu(2) sites where copper atoms are in the  $3d^9$  configuration. The dominant characteristics of the spectrum is the overlapping of different lines corresponding to several Cu(2) sites with a maximum of amplitude near 32.5 MHz. It is likely that this frequency corresponds to the extra peak observed in the Cu(2) site spectrum of the  $\text{LaBa}_2\text{Cu}_3\text{O}_{6+x}$  system with  $x=6.93$  [see Fig. 7(a)] and  $x=7.06$ ,<sup>21</sup> when compared to the  $\text{YBa}_2\text{Cu}_3\text{O}_7$  compound. It can be tentatively attributed to Cu(2) sites just above Cu(1) sites surrounded by oxygen in the O(5) site which are present in  $\text{LaBa}_2\text{Cu}_3\text{O}_{7.05}$ . The best fit of this part of the spectrum, obtained using Gaussian line shapes with the appropriate ratio for the amplitude and the frequencies corresponding to the two Cu isotopes is shown in Fig. 7(c). A set of weak  $^{63}\text{Cu}$ - $^{65}\text{Cu}$  resonance at 26.5 MHz and 28.6 MHz overlaps with a stronger set at 32.4 and 30 MHz and a sharp set at 35 and 32 MHz. These three subsets of lines correspond to Cu(2) sites above Cu(1) sites with different oxygen environments that we can tentatively assign to  $\text{Cu}(1)_3$ ,  $\text{Cu}(1)_5$  with oxygen neighbors in the O(5) sites and  $\text{Cu}(1)_4$ . It is not possible, through this indirect effect on the structure of the Cu(2) spectrum, to go into more details on the possible configurations of the  $\text{Cu}(1)_4$  and  $\text{Cu}(1)_5$  environment in the presence of oxygen atoms on the O(5) sites [like  $\text{Cu}(1)_4$  with two O(4), one O(1) and one O(5) oxygen neighbors and  $\text{Cu}(1)_5$  with two O(4), two O(1) and one O(5) oxygen neighbors]. Nevertheless, the amplitude of the lines set at 32.5 MHz and 30 MHz is consistent with a strong occupancy of the O(5) sites. The low frequency part of the spectrum 20–26 MHz corresponds to Cu(1) sites with copper in the  $3d^9$  configuration. A large broadening with several lines overlapping each other is observed in contrast with the Cu(1) respective line shapes observed in  $\text{LaBa}_2\text{Cu}_3\text{O}_{7.05}$ . The poor resolution of the spectrum due to the extreme sensitivity of the Cu(1) EFG to structural disorder does not allow the identification of the different oxygen environments for the Cu(1) sites. This broad spectrum is however consistent with the presence of three different Cu(1) sites corresponding respectively to the three sets of Cu(2) lines at higher frequencies. The larger weight observed in the  $\text{La}_{1.3}\text{Ba}_{1.7}\text{Cu}_3\text{O}_{7+\delta}$  spectrum around 23 MHz when compared to the  $\text{LaBa}_2\text{Cu}_3\text{O}_{7.05}$  spectrum can be explained by a  $^{63}\text{Cu}$ - $^{65}\text{Cu}$  line set corresponding to the contribution of Cu(1) sites surrounded by O(5) oxygen atoms. Finally the comparison between the copper NQR spectrum of  $\text{LaBa}_2\text{Cu}_3\text{O}_{7.05}$  and of  $\text{La}_{1.3}\text{Ba}_{1.7}\text{Cu}_3\text{O}_{7+\delta}$  evidences the increasing occupancy of O(5) sites with  $x$  in the chain layers. It is also interesting to note that when the crystallographic structure changes from orthorhombic to tetragonal,<sup>28</sup> the Cu(1) and Cu(2) lines shift in opposite directions, which is consistent with the respective evolution of the Cu(1)-O(4) and Cu(2)-O(4) distances.

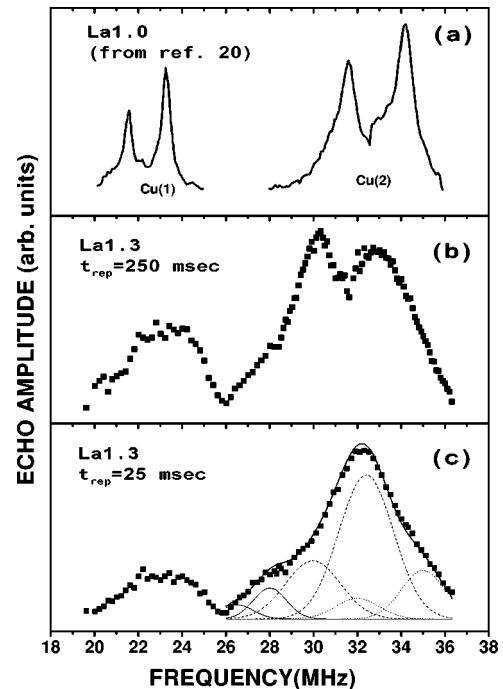


FIG. 7.  $^{63,65}\text{Cu}(1)$  and  $\text{Cu}(2)$  NQR spectra at 4.2 K respectively in (a)  $\text{LaBa}_2\text{Cu}_3\text{O}_{6.93}$  ( $\text{La}1.0$ ) from the data of Lütgmeier *et al.* (Ref. 20), (b)  $\text{La}_{1.3}\text{Ba}_{1.7}\text{Cu}_3\text{O}_{7+\delta}$  ( $\text{La}1.3$ ) with a pulse sequence repetition rate  $t_r=250$  msec, and (c)  $\text{La}_{1.3}\text{Ba}_{1.7}\text{Cu}_3\text{O}_{7+\delta}$  with  $t_r=25$  msec. The solid line represents the fit of the part of the spectrum assigned to the Cu(2) sites (see text) and dotted lines show the three sets of Gaussian line shapes corresponding to the  $^{63,65}\text{Cu}$  isotopes for the three unequivalent Cu(2) sites.

The NQR spectrum of  $\text{Pr}_{1.3}\text{Ba}_{1.7}\text{Cu}_3\text{O}_{7+\delta}$  obtained using a fast repetition rate (25 msec) is represented in Fig. 6. Its analysis is now easier in light of the previous investigation on  $\text{La}_{1.3}\text{Ba}_{1.7}\text{Cu}_3\text{O}_{7+\delta}$ . The low frequency part corresponding to the  $3d^9$  Cu(1) sites is quite similar for the two compounds and reveals the presence of  $\text{Cu}(1)_3$ ,  $\text{Cu}(1)_4$  and  $\text{Cu}(1)_5$  sites, the latter being surrounded by oxygen atoms in the O(5) sites. This indicates that  $\text{La}^{3+}$  and  $\text{Pr}^{3+}$  substitutions on the  $\text{Ba}^{2+}$  sites induce a similar disorder including a charge compensation by O(5) oxygen sites occupancy. The absence of shift and of additional broadening in the Cu(1) spectrum of the Pr compound compared to that of the La compound, indicates that no hyperfine field is transferred due to magnetic  $\text{Pr}^{3+}$  ions even at low temperature. Such a field would be present if any local magnetic order was effective on the substituted Pr sublattice.

The higher frequency part of the spectrum (26–38 MHz) is the most remarkable result of those measurements as it shows the presence of  $3d^9$  copper on the Cu(2) sites of the  $\text{CuO}_2$  planes which are largely dominated by AF order with  $T_N=285$  K. The frequency range of these  $^{63,65}\text{Cu}$  nuclei is a clear signature of metallic copper among the Cu(2) sites. Indeed their frequency range is compatible with the different site assignment made in  $\text{La}_{1.3}\text{Ba}_{1.7}\text{Cu}_3\text{O}_{7+\delta}$  for the superconducting Cu(2) lines. The low signal to noise ratio did not allow a significant measurement of the spin-spin relaxation time in order to give a safe estimation of the relative weight for the sites occupancy. However, a comparison of the NQR signal intensities (in the 32–36 MHz frequency range) in the

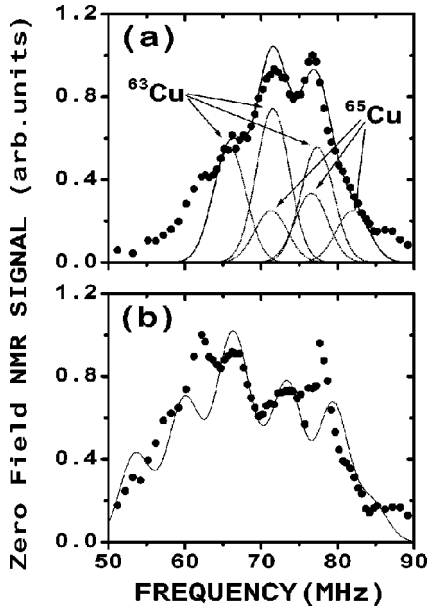


FIG. 8. (a)  $^{63,65}\text{Cu}(2)$  zero-field NMR spectra at 1.8 K in  $\text{Pr}_{1.3}\text{Ba}_2\text{Cu}_3\text{O}_7$ . Dashed curves correspond to quadrupole-split  $^{63,65}\text{Cu}$  lines, simulated with parameters given in Table I. The solid line displays the whole corresponding spectrum. (b)  $^{63,65}\text{Cu}(2)$  zero-field NMR spectra at 1.8 K in  $\text{Pr}_{1.3}\text{Ba}_2\text{Cu}_3\text{O}_{6.9}$ ; the solid line is simulated with parameters given in Ref. 30.

$\text{La}_{1.3}\text{Ba}_{1.7}\text{Cu}_3\text{O}_{7+\delta}$  and  $\text{Pr}_{1.3}\text{Ba}_{1.7}\text{Cu}_3\text{O}_{7+\delta}$  samples gives a rough estimate of the superconducting fraction of 2%. This small fraction is in agreement with the order of magnitude deduced from the susceptibility measurements.

### C. $^{63,65}\text{Cu}$ zero-field NMR

#### 1. The magnetic Cu(2) plane sites spectrum in $\text{PrBa}_2\text{Cu}_3\text{O}_{7-\delta}$ as a function of $\delta$

Before investigating the enhanced Pr substitution effect in  $\text{Pr}_{1.3}\text{Ba}_{1.7}\text{Cu}_3\text{O}_{7+\delta}$ , we have carefully studied the zero field NMR spectrum of the stoichiometric compound ( $x=0$ ) with a particular attention concerning the role of the oxygen concentration upon the magnetic AF order in the  $\text{CuO}_2$  planes. Figure 8 shows the zero-field NMR spectra of the Cu(2) sites in  $\text{PrBa}_2\text{Cu}_3\text{O}_7$  (A, fully oxygenated) and  $\text{PrBa}_2\text{Cu}_3\text{O}_{y\approx 6.9}$  (B, oxygen depleted), whereas Fig. 9 presents the results in  $\text{Pr}_{1.3}\text{Ba}_{1.7}\text{Cu}_3\text{O}_{7+\delta}$ . In the case of copper with a nuclear spin  $I=3/2$ , six peaks are expected in the zero-field NMR spectrum resulting from the quadrupolar splitting of  $^{63}\text{Cu}$  and  $^{65}\text{Cu}$  Zeeman levels. These lines generally overlap each other, with amplitudes and frequencies that depend on the relative values of  $H_{\text{int}}$  and  $\nu_Q$ , and at most six well resolved peaks are obtained.

In the fully oxygenated  $\text{PrBa}_2\text{Cu}_3\text{O}_7$  sample [Fig. 8(a)], the fitting of the spectrum to the hyperfine parameters ( $^{63}\nu_Q$ ,  $H_{\text{int}}$ , and  $\theta$ ) was made assuming that the Cu(2) value of the EFG asymmetry parameter  $\eta$  was equal to zero, as in previous studies in  $\text{PrBa}_2\text{Cu}_3\text{O}_{6+\delta}$ . We obtained  $H_{\text{int}}=63$  kOe, which agrees well with a previous study by Reyes *et al.*<sup>33</sup> It is interesting to compare this value with those reported in the literature for  $\text{RBa}_2\text{Cu}_3\text{O}_{6+\delta}$  (see Table I). In the case of the insulating compound  $\text{PrBa}_2\text{Cu}_3\text{O}_6$ , the usual value is similar to those reported for  $\text{YBa}_2\text{Cu}_3\text{O}_6$  ( $\approx 80$  kOe). In contrast,

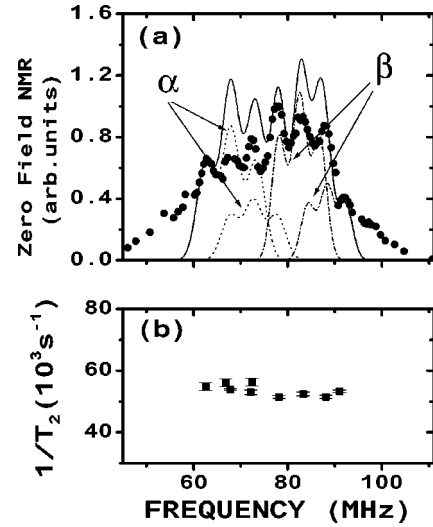


FIG. 9. (a)  $^{63,65}\text{Cu}(2)$  zero-field NMR spectrum at 1.8 K in  $\text{Pr}_{1.3}\text{Ba}_{1.7}\text{Cu}_3\text{O}_{7+\delta}$ ; (b) spin-spin nuclear relaxation rate  $1/T_2$  vs temperature at 1.8 K in  $\text{Pr}_{1.3}\text{Ba}_{1.7}\text{Cu}_3\text{O}_{7+\delta}$ . Dashed curves and dashed-dot curves represent respectively the  $\alpha$  phase and  $\beta$  phase  $^{63,65}\text{Cu}$  lines, simulated with parameters given in Table II. The solid line displays the whole spectrum.

the low value  $H_{\text{int}} \approx 53-63$  kOe has been reported by many authors<sup>15,30,33</sup> for  $\text{PrBa}_2\text{Cu}_3\text{O}_7$ . The AF states in  $\text{PrBa}_2\text{Cu}_3\text{O}_7$  and in  $\text{YBa}_2\text{Cu}_3\text{O}_6$  are very different. It is likely that the hole localization models for  $\text{PrBa}_2\text{Cu}_3\text{O}_7$  explain this difference. Furthermore, this rules out the hypothesis of a pure hole-filling mechanism by  $\text{Pr}^{4+}$ , as one would expect the same AF ordering as in  $\text{YBa}_2\text{Cu}_3\text{O}_6$  in this case.

As emphasized by Nehrke *et al.*,<sup>30</sup> there are significant differences between the various zero-field NMR spectra reported by many authors for  $\text{PrBa}_2\text{Cu}_3\text{O}_7$ . Assuming a lowering of Pr point symmetry, Nehrke *et al.* deduced two types of Cu(2) site in  $\text{PrBa}_2\text{Cu}_3\text{O}_{6+\delta}$ . They used two different hyperfine fields values to fit their data, as shown in Table I. Nevertheless, they were not able to make a clear distinction between this approach and the traditional assumption of a unique Cu(2) site. Our spectrum obtained in a fully oxygenated sample  $\text{PrBa}_2\text{Cu}_3\text{O}_7$  does not reproduce the feature of

TABLE I. Cu(2) hyperfine field  $H_{\text{int}}$ , nuclear quadrupole frequency  $^{63}\nu_Q$ , and angle  $\theta$  between the  $c$  axis and  $H_{\text{int}}$ , extracted from zero-field NMR data in  $\text{Y}_1\text{Ba}_2\text{Cu}_3\text{O}_6$ ,  $\text{GdBa}_2\text{Cu}_3\text{O}_6$ , and in  $\text{Pr}_1\text{Ba}_2\text{Cu}_3\text{O}_{6+\delta}$ .

Sample	$H_{\text{int}}$ (kOe)	$^{63}\nu_Q$ (MHz)	$\theta$ (deg)	Reference
$\text{YBa}_2\text{Cu}_3\text{O}_6$	79	22	90	16
$\text{GdBa}_2\text{Cu}_3\text{O}_6$	$76.7 \pm 1.5$	25	90	30
$\text{PrBa}_2\text{Cu}_3\text{O}_6$	78	13–16	75–90	15
$\text{PrBa}_2\text{Cu}_3\text{O}_6$	$73 \pm 3$	4–15	90	30
	$85 \pm 3$	4–15	90	
$\text{PrBa}_2\text{Cu}_3\text{O}_7$	59	18–20	75–90	15
$\text{PrBa}_2\text{Cu}_3\text{O}_7$	$65 \pm 2$	$17.2 \pm 1.5$	$78.8 \pm 1.1$	33
$\text{PrBa}_2\text{Cu}_3\text{O}_7$	$53 \pm 3$	$\approx 12.7$	90	Ref. 30
	$65 \pm 3$	$\approx 12.7$	90	
$\text{PrBa}_2\text{Cu}_3\text{O}_7$	$63 \pm 1$	$14.5 \pm 1$	$75 \pm 5$	Present work

TABLE II. Cu(2) zero-field NMR parameters  $H_{\text{int}}$ ,  ${}^{63}\nu_Q$ ,  $\theta$ , and Cu lines FWHM  $\Gamma$ , for the  $\alpha$  and  $\beta$  phases in  $\text{Pr}_{1.3}\text{Ba}_{1.7}\text{Cu}_3\text{O}_{7+\delta}$ .

Sample		$H_{\text{int}}$ (kOe)	${}^{63}\nu_Q$ (MHz)	$\theta$ (deg)	$\Gamma$ (MHz)
$\text{Pr}_{1.3}\text{Ba}_{1.7}\text{Cu}_3\text{O}_{7+\delta}$	PHASE $\alpha$	$60 \pm 1$	$13.5 \pm 1$	$75 \pm 5$	$3.75 \pm 0.25$
	PHASE $\beta$	$73 \pm 1$	$9.5 \pm 1$	$80 \pm 5$	$3.0 \pm 0.25$

two different Cu(2) sites, and only one hyperfine field was used to simulate it, as in previous studies by Yoshimura *et al.*<sup>15</sup> and Reyes *et al.*<sup>33</sup> Suspecting some significant differences between the samples due to variations in the conditions of synthesis, such as the degree of Ba substitution by Pr or the oxygen stoichiometry, we studied the zero-field NMR spectrum of a slightly oxygen-depleted sample  $\text{PrBa}_{2-x}\text{Cu}_3\text{O}_{y \approx 6.9}$ . We obtained a spectrum [see Fig. 8(b)] that is very similar to that reported by Nehrke *et al.*, and we simulated it well using the parameter values given in their paper.<sup>30</sup> This result calls for a careful analysis of the zero-field NMR data in nonstoichiometric samples, and demonstrates that chain structure and defects strongly affect the magnetic ordering of the  $\text{CuO}_2$  planes.

## 2. The magnetic Cu(2) plane sites in $\text{Pr}_{1.3}\text{Ba}_{1.7}\text{Cu}_3\text{O}_{7+\delta}$

In the  $\text{Pr}_{1.3}\text{Ba}_{1.7}\text{Cu}_3\text{O}_{7+\delta}$  zero-field NMR spectrum shown in Fig. 9(a), the line shape displays an unusual structure, with *seven well-resolved peaks* between 45 MHz and 110 MHz. No consistent solution to fit this line shape with only one set of hyperfine parameters  $H_{\text{int}}$ ,  ${}^{63}\nu_Q$ , and  $\theta$  was found. We conclude that there are two types of Cu(2) sites in our sample, with different hyperfine field parameters. At this stage, it is important to rule out the possibility of a parasitic phase in our sample. We therefore measured the nuclear spin-spin relaxation rate at 1.8 K [Fig. 9(b)], and found a roughly constant value in the whole frequency range,  $1/T_2 \approx 54 \pm 2.5$  kHz. Thus, our results exclude the impurity hypothesis as (i) all the nuclear spins are connected by the same spin-spin interaction ( $1/T_2$  is constant), (ii) we detected no parasitic phase in the x-ray diffraction pattern (with a typical threshold of 1%), and (iii) the relative amplitudes of the peaks are not consistent with such a phase, as one would expect a smaller amplitude for the parasitic phase peaks. We therefore used two sets of hyperfine field parameters to fit our data:  $H_{\text{int}}^\alpha$ ,  ${}^{63}\nu_Q^\alpha$ , and  $\theta^\alpha$  for the low frequency part of the line shape and  $H_{\text{int}}^\beta$ ,  ${}^{63}\nu_Q^\beta$ , and  $\theta^\beta$  for the high frequency part, the labels  $\alpha$  and  $\beta$  referring to the two distinct magnetic phases. The parameters of the  $\alpha$  phase (see Table II) are very close to those we reported for  $\text{Pr}_1\text{Ba}_2\text{Cu}_3\text{O}_7$  while those of the  $\beta$  phase are closer to those reported for  $\text{Pr}_1\text{Ba}_2\text{Cu}_3\text{O}_6$  in other studies.

Another key parameter for the understanding of the in-plane electronic state is given by the Cu(2) quadrupolar splitting, deduced from the fit of the zero-field NMR spectra. Yoshimura *et al.*<sup>15</sup> compared the  ${}^{63}\nu_Q$  found in  $\text{PrBa}_2\text{Cu}_3\text{O}_{6+\delta}$  for  $\delta=0$  and  $\delta=1$  with  ${}^{63}\nu_Q$  in other  $R\text{Ba}_2\text{Cu}_3\text{O}_{6+\delta}$  systems. To analyze their results, they used the simple phenomenological model proposed by Shimizu<sup>18</sup>, in which

$${}^{63}\nu_Q = A e q_{\text{latt}} + B, \quad (6)$$

where  $e q_{\text{latt}}$  is the lattice contribution to the EFG ( $A$  is a scaling factor related to the Sternheimer antishielding factor), and  $B$  is an on-site contribution due to  $3d$  electronic orbitals of the Cu ion. From their calculations, Yoshimura *et al.* claimed that the scaling factor  $A$  was the same in  $\text{YBa}_2\text{Cu}_3\text{O}_{6+\delta}$  and  $\text{PrBa}_2\text{Cu}_3\text{O}_{6+\delta}$ , but that the on-site contribution  $B$  was markedly different in the two structures. Indeed, the Cu(2) quadrupolar frequency is anomalously low in the Pr-123 structure, compared to the Y-123 system. The contribution of the Cu wave function to the quadrupole interaction was found to be reduced in the Pr system, which was related to Pr-O-Cu hybridization and to in-plane hole localization. In the particular case of  $\text{Pr}_{1.3}\text{Ba}_{1.7}\text{Cu}_3\text{O}_{7+\delta}$ , we found for the two phases respectively  ${}^{63}\nu_Q^\alpha = 13.5$  MHz and  ${}^{63}\nu_Q^\beta = 9.5$  MHz. The  $\alpha$  phase value is roughly the same as that we give for  $\text{PrBa}_2\text{Cu}_3\text{O}_7$  ( ${}^{63}\nu_Q = 14.5$  MHz), whereas the smaller  $\beta$  value is consistent with a local EFG similar to the  $\text{PrBa}_2\text{Cu}_3\text{O}_6$  situation.

In conclusion, the zero-field NMR spectrum in  $\text{Pr}_{1.3}\text{Ba}_{1.7}\text{Cu}_3\text{O}_{7+\delta}$  gives evidence for a phase separation in the sample. Some Cu(2) sites are located in domains (the  $\alpha$  phase) where the hyperfine parameters are similar to that found in well-ordered  $\text{PrBa}_2\text{Cu}_3\text{O}_7$ , whereas a second phase (the  $\beta$  phase) reflects the existence of domains reminiscent of the  $\text{CuO}_2$  planes in nondoped  $\text{PrBa}_2\text{Cu}_3\text{O}_6$ .

## V. DISCUSSION

A common feature reported in the previous studies on nonstoichiometric  $R_{1+x}\text{Ba}_{2-x}\text{Cu}_3\text{O}_{7+\delta}$  systems (with  $R=\text{La, Nd, Pr}$ ) is the disorder present in the chain layers and the occupancy of O(5) interchain sites. Though the observed superconducting state in this study for  $R=\text{Pr}$  is anomalous, the mechanisms which perturb the crystallographic structure and the chain to plane hole transfer are similar whatever the rare earth element is. In this context it is important to carefully compare the case of  $\text{La}_{1+x}\text{Ba}_{2-x}\text{Cu}_3\text{O}_{7+\delta}$  and  $\text{Nd}_{1+x}\text{Ba}_{2-x}\text{Cu}_3\text{O}_{7+\delta}$  systems where the  $\text{Ba}^{2+}/\text{R}^{3+}$  substitution depresses the superconducting properties, with the case of  $\text{Pr}_{1+x}\text{Ba}_{2-x}\text{Cu}_3\text{O}_{7+\delta}$  where a small superconducting fraction appears as a function of the substitution rate  $x$ . We will discuss our results on the latter compounds in the light of the information available on the former compounds, and we will show that the same basic mechanisms are to be considered.

### A. Structural effects due to the $R^{3+}$ substitution for $\text{Ba}^{2+}$ in $R_{1+x}\text{Ba}_{2-x}\text{Cu}_3\text{O}_{7+\delta}$ ( $R=\text{La, Nd, and Pr}$ )

The substitution of trivalent  $R$  ions on the Ba sites is particularly important in the  $R\text{Ba}_2\text{Cu}_3\text{O}_7$  cuprates when the rare earth atomic radius is large as in the case of La, Nd, and



Pr. For these three rare earth based compounds, the structural changes observed by x-ray and neutron diffraction measurements as a function of  $x$  are similar and show a progressive reduction in the orthorhombicity of the structure due to the O(5) sites occupancy.<sup>29,34,28,35</sup> An orthorhombic to tetragonal transition arises for substitution rates  $x$  between 0.1 and 0.2. For a moderate substitution rate, according to the chemical bonding in the chain layers, the extra oxygen O<sup>2-</sup> ions occupying the O(5) sites prevent the charge unbalance generated by the trivalent R<sup>3+</sup> ions on the Ba<sup>2+</sup> sites. Nevertheless, for large values of  $x$ , the charge balance is no longer preserved as the excess of oxygen saturates: the copper chain valence is therefore modified.

**B. Effect of La<sup>3+</sup> and Nd<sup>3+</sup> substitution for Ba<sup>2+</sup> on the charge transfer and the superconducting properties in La<sub>1+x</sub>Ba<sub>2-x</sub>Cu<sub>3</sub>O<sub>7+δ</sub> and Nd<sub>1+x</sub>Ba<sub>2-x</sub>Cu<sub>3</sub>O<sub>7+δ</sub> systems**

When La and Nd are substituted for Ba in the R<sub>1+x</sub>Ba<sub>2-x</sub>Cu<sub>3</sub>O<sub>7+δ</sub> system, the  $T_c$  is smoothly depressed for  $x < 0.2$  and decreases with a larger slew rate for  $x > 0.2$ . A large reduction in the screening fraction is also observed as  $x$  increases.<sup>29</sup> The last point clearly indicates that the corresponding superconducting state is inhomogeneous. For large values of  $x$  the  $T_c$  diminution is well understood as arising from a hole-depletion due to the charge unbalance generated by R<sup>3+</sup>/Ba<sup>2+</sup> substitution. Nevertheless, for moderate values of  $x$ , this simple picture fails to consistently account for the decrease in  $T_c$  and in the screening fractions. To illustrate this point, if we consider the oxygen content  $\Delta(x) = 7 + \delta$  in Nd<sub>1+x</sub>Ba<sub>2-x</sub>Cu<sub>3</sub>O<sub>7+δ</sub> deduced from the data of Kramer *et al.*,<sup>29</sup> a simple application of the charge balance rules would give for  $x < 0.3$  a plane hole-doping quite constant and therefore a value of  $T_c$  roughly unaffected.<sup>36</sup> A better understanding of the  $T_c$  variation with  $x$  is achieved, taking into account the local inhibition of the charge transfer by the disorder introduced in the charge reservoir layer. For small values of  $x$ , the degree of disorder is weak and the charge balance is preserved by the presence of O(5) oxygen atoms. Such a situation corresponds to a smoothly reduced value of  $T_c$  as observed experimentally in La<sub>1.1</sub>Ba<sub>1.9</sub>Cu<sub>3</sub>O<sub>7+δ</sub> (Ref. 35) and Nd<sub>1.12</sub>Ba<sub>1.88</sub>Cu<sub>3</sub>O<sub>7+δ</sub>,<sup>37</sup> where  $T_c \cong 90$  K. For higher substitution rate values, the disorder increases and the value of the excess of oxygen  $\delta$  saturates: as a result, the charge transfer between chains and planes is locally suppressed, in the vicinity of the most strongly perturbed chain sites. The simultaneous reduction in the screening fractions and in the  $T_c$  reported by several authors is therefore better explained, considering a progressive growth of insulating areas inside the superconducting planes rather than taking into account a simple homogeneous decrease in the hole doping. The fraction of these insulating areas which corresponds to local perturbations of the charge reservoir increases with  $x$ , and the superconducting regions become coupled through weak links. This situation is similar to that described by Muroi *et al.*<sup>14</sup> in the Y<sub>1-x</sub>Pr<sub>x</sub>Ba<sub>2-y</sub>Sr<sub>y</sub>Cu<sub>3</sub>O<sub>7</sub> system and results in an inhomogeneous character of the superconducting state. The systematic decrease in Meissner fraction with increasing  $x$  reported by Kramer *et al.*<sup>38</sup> in Nd<sub>1+x</sub>Ba<sub>2-x</sub>Cu<sub>3</sub>O<sub>7+δ</sub> supports this picture. Finally we must point out the importance

of the synthesis conditions of the R<sub>1+x</sub>Ba<sub>2-x</sub>Cu<sub>3</sub>O<sub>7+δ</sub> samples which govern the O(5) site occupancy and the statistics of the distribution of the substituted Ba sites. With respect to the last point, a tendency for there to be a pairing of substituted Nd on adjacent Ba sites was noted by Kramer *et al.*<sup>38</sup> in Nd<sub>1+x</sub>Ba<sub>2-x</sub>Cu<sub>3</sub>O<sub>7+δ</sub>. Using electron diffraction which provides a high degree of spatial resolution, they have shown that for  $x > 0.25$ , an increasing number of substituted Nd atoms were adjacent to other substituted Nd atoms. This situation keeps a local charge balance with one O on the intermediate O(5) site and increases the number of fourfold coordinated Cu's on the chain which governs the charge transfer. For a given substitution rate, these parameters strongly depend on the sample preparation conditions such as the temperature or the oxygen partial pressure. As an example, Salluzzo *et al.*<sup>37</sup> observed a  $T_c = 90$  K in Nd<sub>1.12</sub>Ba<sub>1.88</sub>Cu<sub>3</sub>O<sub>7+δ</sub> when for the same substitution level, Kramer *et al.*<sup>38</sup> claimed a  $T_c$  value of 50–60 K.

**C. Effect of Pr<sup>3+</sup> substitution for Ba<sup>2+</sup> on the charge transfer in Pr<sub>1+x</sub>Ba<sub>2-x</sub>Cu<sub>3</sub>O<sub>7+δ</sub>**

Our NQR data on the Cu(1) chain sites in PrBa<sub>2</sub>Cu<sub>3</sub>O<sub>7</sub> show that the doping of the chains and consequently the charge transfer are the same as for YBa<sub>2</sub>Cu<sub>3</sub>O<sub>7</sub>. The major difference with this last compound is the hole localization through Pr<sub>4f</sub>-O<sub>2p</sub> orbitals hybridization. This hybridization is mainly oriented along the  $b$ -axis (chain direction) as shown in PrBa<sub>2</sub>Cu<sub>3</sub>O<sub>7</sub> orthorhombic samples by neutron diffraction studies<sup>39</sup> and NMR measurements of the electric field gradient at the oxygen plane sites.<sup>6</sup>

The Cu(1) NQR spectrum evolution which is observed in Pr<sub>1.3</sub>Ba<sub>1.7</sub>Cu<sub>3</sub>O<sub>7+δ</sub> confirms the disorder introduced in the charge reservoir layer by the O(5) site occupancy as in La<sub>1.3</sub>Ba<sub>1.7</sub>Cu<sub>3</sub>O<sub>7+δ</sub>. The implications of this disorder on the magnetism of copper in the Cu(2) plane sites are probed by the <sup>63,65</sup>Cu zero-field NMR spectrum. This data shows the coexistence of regions without holes (as in PrBa<sub>2</sub>Cu<sub>3</sub>O<sub>6</sub>), with regions in which the holes are localized (as in PrBa<sub>2</sub>Cu<sub>3</sub>O<sub>7</sub>). The first ones are correlated to the presence of a strong perturbation in the charge reservoir and the last ones to clusters where the CuO<sub>3</sub> chains are unperturbed (i.e., the charge transfer is not depressed). Furthermore, the observation of a small superconducting fraction by DC SQUID measurements and the presence of superconducting Cu(2) sites detected by NQR, indicate that regions where holes are mobile also exist.

Let us now discuss the mechanisms which could explain the presence of such mobile holes in the CuO<sub>2</sub> planes. Two fundamental points are to be considered in a crude phenomenological approach. The first one concerns the presence of an effective charge transfer from chains to planes. This mechanism is essentially governed by the presence of fourfold coordinated copper atoms in the chains and is perturbed by oxygen vacancies on the O(1) sites and by the presence of uncompensated oxygen bonding on O(5) sites. The breaking of the Pr<sub>4f</sub>-O<sub>2p</sub> hybridization is the second important point. This orbital bonding which localizes the holes depends on the Pr-O(2,3) atomic distance and also on the local orthorhombic symmetry. In the framework of these two constraints we propose two phenomenological explanations for

the existence of mobile holes in the  $x=0.3$  sample. In a first general approach, if we consider (by analogy with the case of  $\text{La}_{1+x}\text{Ba}_{2-x}\text{Cu}_3\text{O}_{7+\delta}$  and  $\text{Nd}_{1+x}\text{Ba}_{2-x}\text{Cu}_3\text{O}_{7+\delta}$ ) that  $x=0.3$  is slightly over the limit of a moderate substitution rate ( $x=0.2$ ) for which the  $T_c$  depression is not drastic, the presence of undisturbed chain segments where the charge transfer is fully effective becomes highly probable. Furthermore near the frontier of the orthorhombic to tetragonal transition, a local decrease in the orthorhombic symmetry in the basal plane could delocalize the holes in the  $\text{Cu}_{x^2-y^2}\text{-O}_{2p}$  orbitals. We must here emphasize that a natural consequence of the  $\text{Ba}^{2+}/\text{Pr}^{3+}$  substitution is a variation in the positions of the neighbors O(1) and O(4) atoms around the substituted site. A further microscopic approach can be proposed considering the pairing occurrence of adjacent Pr atoms substituted on Ba sites on both sides of  $\text{CuO}_3$  planes as observed experimentally by Kramer *et al.*<sup>38</sup> for Nd atoms in  $\text{Nd}_{1+x}\text{Ba}_{2-x}\text{Cu}_3\text{O}_{7+\delta}$ . This situation keeps the fourfold coordination of copper in the Cu(1) site surrounded by the two adjacent Pr atoms (as explained in the previous section for Nd atoms) and locally increases the distance between Pr (located inside the  $\text{CuO}_2$  bilayers) and the O(2,3) oxygen atoms. This local distortion of the structure contributes to a decrease in the  $\text{Pr}_{4f}\text{-O}_{2p}$  hybridization.

In summary, the three following situations could be present for the copper environment in the chains: (i) the Ba site is not substituted; (ii) the Ba site is substituted by a Pr ion with an extra oxygen atom on the O(5) site; (iii) two Ba sites adjacent to a Cu(1) site are substituted with a single extra oxygen atom on the O(5) site. In the first two cases, independent of the chain to plane charge transfer existence, the  $\text{Pr}_{4f}\text{-O}_{2p}$  hybridization is active and prevents any mobility for holes in the  $\text{CuO}_2$  planes. The last case could correspond to the coexistence of an active charge transfer and the inhibition of the Pr-O hybridization.

#### D. The formation of superconducting clusters in $\text{Pr}_{1+x}\text{Ba}_{2-x}\text{Cu}_3\text{O}_{7+\delta}$

If we compare our experimental results with the data in substituted R-123 systems with  $R=\text{La}$  and  $\text{Nd}$ , some of the features that are observed are similar as to those of the orthorhombic to tetragonal transition for a critical value of  $x$  and of the phase separation which takes place in the  $\text{CuO}_2$  planes, but a strong divergence appears on the evolution of the  $T_c$  as a function of  $x$ . All the superconducting fractions observed in our  $\text{Pr}_{1+x}\text{Ba}_{2-x}\text{Cu}_3\text{O}_{7+\delta}$  samples present a  $T_c=90\text{--}80$  K with a sharp diamagnetic signal. This excludes a percolative nature of the superconducting transition as in granular systems where the  $T_c$  and the width of the transition depends on the weak link bonding.

For a moderate substitution rate, a phase separation on the microscopic scale takes place in the  $\text{CuO}_2$  planes of  $\text{Pr}_{1+x}\text{Ba}_{2-x}\text{Cu}_3\text{O}_{7+\delta}$  systems with a statistic distribution of three characteristic regions which we label respectively ( $\alpha$ ) in which localized holes exist, ( $\beta$ ) without holes, and ( $\gamma$ ) where mobile holes reside. For high substitution rates, the charge transfer is totally inhibited by the large disorder present in the charge reservoir and the  $\text{CuO}_2$  planes remain completely insulating.

If we assume the validity of the mechanisms proposed in the previous section with respect to the origin of mobile holes in the  $\text{CuO}_2$  planes, a last step to understand the signature of the diamagnetic signals observed by DC SQUID measurements concerns the statistics of the substituted sites with different Pr environments. The observation by Kramer *et al.*,<sup>38</sup> using electron energy loss spectroscopy, of a tweed pattern in a  $\text{Nd}_{1.25}\text{Ba}_{1.75}\text{Cu}_3\text{O}_{7+\delta}$  sample, suggests the presence of a local ordering of the substituted  $R^{3+}$  ions in these systems. Such a tendency to segregate into clusters for the substituted Ba sites by Pr increases the probability of finding adjacent  $\text{Pr}^{3+}$  ions forming pairs. It is worth noting that clustering must produce fivefold copper atoms in the Cu(1) sites, a feature which was observed in our NQR spectrum. The size of these clusters is dependent on the degree of local structural distortion. There is however a limit to the distortion that can be obtained before the structure becomes unstable. Nevertheless, when their dimensions reach the critical value corresponding to several time the superconducting correlation length, a superconducting state can be present. Of course, the mechanisms involved in this phenomenological model are very sensitive to the synthesis conditions as the process temperature, the  $\text{O}_2$  partial pressure and the details of the annealing treatments.

As regard to the mechanism of phase separation in cuprates, the coexistence of magnetic and superconducting orders and the interplay between local structural distortion and the presence of the superconducting clusters observed in  $\text{Pr}_{1.3}\text{Ba}_{1.7}\text{Cu}_3\text{O}_{7+\delta}$  present a great interest. There are obvious similarities with the physics of phase separation actively investigated in lanthanum cuprates.<sup>40–43</sup> In these systems were a substantial fraction of the doped holes localize in  $\text{CuO}_2$  planes, a relationship between ordered phase separation (like stripes) and structural features that pin these objects have been demonstrated. Nevertheless, in  $\text{Pr}_{1.3}\text{Ba}_{1.7}\text{Cu}_3\text{O}_{7+\delta}$  the spatial order and the size of the different domains corresponding to the  $\alpha$ ,  $\beta$ , and  $\gamma$  phases remains to be investigated in more detail before going further in the comparison.

## VI. CONCLUSION

The main result of this investigation is the microscopic evidence that the small superconducting fractions observed below 90 K in the  $\text{Pr}_{1+x}\text{Ba}_{2-x}\text{Cu}_3\text{O}_{7+\delta}$  system are induced by the local structural change associated with the substitution of Ba by Pr. We have focused our study on the sample with  $x=0.3$  for which the superconducting fraction was maximum. From copper NQR measurements we show that the hole doping of the chains and the charge transfer between chains and planes is similar for  $\text{YBa}_2\text{Cu}_3\text{O}_7$  and the nonsubstituted compound  $\text{PrBa}_2\text{Cu}_3\text{O}_7$ . The copper chains Cu(1) NQR line shape obtained for  $\text{Pr}_{1.3}\text{Ba}_{1.7}\text{Cu}_3\text{O}_{7+\delta}$  which spreads over a wide frequency range (between 19 and 30 MHz) provides evidence for the disorder introduced in the  $\text{CuO}_3$  chains by oxygen vacancies and the oxygen interchain sites O(5) occupancy resulting from the  $\text{Ba}^{2+}/\text{Pr}^{3+}$  substitution. At higher frequencies, in the 30–39 MHz frequency range, a tiny signal associated with metallic copper on the  $\text{CuO}_2$  plane Cu(2) sites is detected. A comparison between the zero-field NMR spectrum of magnetic Cu(2) sites in

$\text{PrBa}_2\text{Cu}_3\text{O}_7$  and  $\text{Pr}_{1.3}\text{Ba}_{1.7}\text{Cu}_3\text{O}_{7+\delta}$  reveals that  $\text{Ba}^{2+}/\text{Pr}^{3+}$  substitution leads to the existence of two magnetic phases, the  $\alpha$  phase with localized holes (as in  $\text{PrBa}_2\text{Cu}_3\text{O}_7$ ) and the  $\beta$  phase without holes present (as in  $\text{PrBa}_2\text{Cu}_3\text{O}_6$ ). The combination of these results are discussed in terms of a phase separation which takes place in the  $\text{CuO}_2$  planes with a statistic distribution of three characteristic domains: ( $\alpha$ ) in which localized holes are present, ( $\beta$ ) where no holes have been transferred from the chains, and ( $\gamma$ ) presenting mobile holes. The presence of mobile holes is phenomenologically interpreted as resulting from a tendency for the  $\text{Pr}^{3+}$  substituted atoms on the Ba sites to segregate and form pairs around the Cu(1) sites. This locally keeps the charge transfer active and breaks the  $\text{Pr}_{4f}\text{-O}_{2p}$  hybridization. In this model, the weak superconducting fractions observed find their origin

in the existence of such clusters when their size reaches a threshold value corresponding to the existence of several elementary  $\text{CuO}_2$  cells. Further experiments are needed to provide a deeper understanding of the nature of this defect-induced superconductivity, such as varying the oxygen stoichiometry and the synthesis conditions of the samples.

#### ACKNOWLEDGMENTS

The partial support of this work by the DRET, France, Grant No. 94-099, is gratefully acknowledged. The Laboratoire de Spectrométrie Physique is Unité Mixte de Recherche C.N.R.S.(C5588).

- <sup>1</sup>A. Kebede, C. S. Jee, J. Schwegler, J. E. Crow, T. Mihalisin, G. H. Myer, M. V. Kuric, S. H. Bloom, and R. P. Guertin, *Phys. Rev. B* **40**, 4453 (1989).
- <sup>2</sup>H.A. Blackstead and J.D. Dow, *Phys. Rev. B* **51**, 11 830 (1995).
- <sup>3</sup>R. Fehrenbacher and T.M. Rice, *Phys. Rev. Lett.* **70**, 3471 (1993).
- <sup>4</sup>A.I. Liechtenstein and I.I. Mazin, *Phys. Rev. Lett.* **74**, 1000 (1995).
- <sup>5</sup>M. Merz, N. Nücker, E. Pellegrin, P. Schweiss, S. Schuppler, M. Kielwein, M. Knupfer, M. S. Golden, J. Fink, C. T. Chen, V. Chakarian, Y. U. Idzerda, and A. Erb, *Phys. Rev. B* **55**, 9160 (1997).
- <sup>6</sup>Y. H. Ko, H. K. Kweon, H. C. Lee, and N. H. Hur, *Physica C* **224**, 357 (1994).
- <sup>7</sup>M. Takata, T. Takayama, M. Sakata, S. Sasaki, K. Kodama, and M. Sato, *Physica C* **263**, 340 (1996).
- <sup>8</sup>H.A. Blackstead, J.D. Dow, D.B. Chrisey, J.S. Horwitz, M.A. Black, P.J. McGinn, A.E. Klunzinger, and D.B. Pulling, *Phys. Rev. B* **54**, 6122 (1996).
- <sup>9</sup>T. Usagawa, Y. Ishimaru, J. Wan, T. Utagawa, S. Koyama, and Y. Enomoto, *Jpn. J. Appl. Phys., Part 2* **36**, L1583 (1997).
- <sup>10</sup>Z. Zou, J. Ye, K. Oka, and Y. Nishihara, *Phys. Rev. Lett.* **80**, 1074 (1998).
- <sup>11</sup>A. Shukla, B. Barbiellini, A. Erb, A. Manuel, T. Buslaps, V. Honkimäki, and P. Suortti, *Phys. Rev. B* **59**, 12 127 (1999).
- <sup>12</sup>J. Ye, Z. Zou, A. Matsushita, K. Oka, Y. Nishihara, and T. Matsumoto, *Phys. Rev. B* **58**, R619 (1998).
- <sup>13</sup>G. Cao, Y. Qian, X. Li, Z. Chen, C. Wang, K. Ruan, Y. Qiu, L. Cao, Y. Ge, and Y. Zhang, *J. Phys.: Condens. Matter* **7**, L287 (1995).
- <sup>14</sup>M. Muroi and R. Street, *Physica C* **301**, 277 (1998).
- <sup>15</sup>Yoshimura, N. Saga, T. Sawamura, M. Kato, T. Shimizu, and K. Kosuge, *Physica C* **235**, 1701 (1994).
- <sup>16</sup>H. Yasuoka, in *Mechanisms of High Temperature Superconductivity*, edited by H. Kamimura and A. Oshiyama, Springer Series in Material Science Vol. 11 (Springer, New York, 1989), p. 156.
- <sup>17</sup>P. Mendels, H. Alloul, J.F. Marucco, J. Arabski, and G. Collin, *Physica C* **171**, 429 (1990).
- <sup>18</sup>T. Shimizu, *J. Phys. Soc. Jpn.* **62**, 772 (1993).
- <sup>19</sup>A. J. Vega, W. E. Farneth, E. M. McCarron, and R. K. Bordia, *Phys. Rev. B* **39**, 2322 (1989).
- <sup>20</sup>H. Lütgemeier, S. Schmenn, P. Meuffels, O. Storz, R. Schöllhorn, C. Niedermayer, I. Heinmaa, and Y. Baikov, *Physica C* **267**, 191 (1996).
- <sup>21</sup>A. Goto, H. Yasuoka, K. Otzsch, and Y. Ueda, *Phys. Rev. B* **55**, 12 736 (1997).
- <sup>22</sup>P. Blaha, K. Schwarz, and P. Herzig, *Phys. Rev. Lett.* **54**, 1192 (1985).
- <sup>23</sup>K. Schwarz, C. Ambrosch-Draxl, and P. Blaha, *Phys. Rev. B* **42**, 2051 (1990).
- <sup>24</sup>C. Ambrosch-Draxl, P. Blaha, and K. Schwarz, *Phys. Rev. B* **44**, 5141 (1991).
- <sup>25</sup>G. Zheng, Y. Kitaoka, K. Ishida, and K. Asayama, *J. Phys. Soc. Jpn.* **64**, 2524 (1995).
- <sup>26</sup>M. Takigawa, N. Motoyama, H. Eisaki, and S. Uchida (private communication).
- <sup>27</sup>B. Grévin, Y. Berthier, G. Collin, and P. Mendels, *Phys. Rev. Lett.* **80**, 2405 (1998).
- <sup>28</sup>S.K. Malik, R. Prasad, N.C. Soni, K. Adhikary, and W.B. Yelon, *Physica B* **223**, 562 (1996).
- <sup>29</sup>M. J. Kramer, K. W. Dennis, D. Falzgraf, R. W. McCallum, S. K. Malik, and W. B. Yelon, *Phys. Rev. B* **56**, 5512 (1997).
- <sup>30</sup>K. Nehrke, M.W. Pieper, and T. Wolf, *Phys. Rev. B* **53**, 229 (1996).
- <sup>31</sup>L. Hoffmann, A. A. Manuel, M. Peter, E. Walker, M. Gauthier, A. Shukla, B. Barbiellini, S. Massidda, Gh. Adam, S. Adam, W. N. Hardy, and R. Liang, *Phys. Rev. Lett.* **71**, 4047 (1993).
- <sup>32</sup>K. Takenaka, Y. Imanaka, K. Tamasaku, T. Ito, and S. Uchida, *Phys. Rev. B* **46**, 5833 (1992).
- <sup>33</sup>A.P. Reyes, D.E. MacLaughlin, M. Takigawa, P.C. Hammel, R.H. Heffner, J.D. Thompson, J.E. Crow, A. Kebede, T. Mihalisin, and J. Schwegler, *Phys. Rev. B* **42**, 2688 (1990).
- <sup>34</sup>G. Collin, A.C. Audier, P.A. Albouy, S. Senoussi, R. Comes, M. Konczykowski, and F. Rullier-Albenque, *J. Phys. (France)* **50**, 77 (1989).
- <sup>35</sup>T. Wada, N. Suzuki, S. Uchida, and S. Tanaka, *Phys. Rev. B* **39**, 9126 (1989).
- <sup>36</sup>B. Grévin, thesis, University of Grenoble, 1998.
- <sup>37</sup>M. Salluzzo, I. Maggio-Aprile, and O. Fischer, *Appl. Phys. Lett.* **73**, 683 (1998).
- <sup>38</sup>M.J. Kramer, S.I. Yoo, R.W. McCallum, W.B. Yelon, H. Xie, and P. Allenspach, *Physica C* **219**, 145 (1994).
- <sup>39</sup>M. Guillaume, P. Allenspach, W. Henggeler, J. Mesot, B. Roessli, U. Staub, P. Fischer, A. Furrer, and V. Trounov, J.

- Phys.: Condens. Matter **6**, 7963 (1994).
- <sup>40</sup>P.C. Hammel, A.P. Reyes, S.-W. Cheong, Z. Fisk, and J.E. Schirber, Phys. Rev. Lett. **71**, 440 (1993).
- <sup>41</sup>B.W. Statt, P.C. Hammel, Z. Fisk, S.-W. Cheong, F.C. Chou, D.C. Johnston, and J. E. Schirber, Phys. Rev. B **52**, 15 575 (1995).
- <sup>42</sup>P.C. Hammel, B.W. Statt, R.L. Martin, F.C. Chou, D.C. Johnson, and S.W. Cheong, Phys. Rev. B **57**, R712 (1998).
- <sup>43</sup>M.-H. Julien, F. Borsa, P. Carretta, M. Horvatic, C. Berthier, and C.T. Lin, Phys. Rev. Lett. **83**, 604 (1999).